RESEARCH PAPER

Computational Investigation of Bioactive Compounds from *Hibiscus sabdariffa* in Modulating TGA Biosynthesis: An Approach to Control Obesity

Sweta Sharma[1*], Swapna Kumar Srivastava[1], Rashi Srivastava[1]
[1]School of Biotechnology, IFTM University, Moradabad, U.P.

ABSTRACT
Diacylglycerol acyltransferase catalyzes the terminal, rate-limiting step of acyl-CoA-dependent triglyceride synthesis, mediating the conversion of diacylglycerol and acyl-CoA into triglycerides. This study aims to identify safer natural therapeutic alternatives by computationally screening the bioactive constituents of *Hibiscus sabdariffa* for their capacity to attenuate the triglyceride biosynthetic pathway through targeted inhibition of DGAT. A comprehensive computational framework, incorporating molecular docking, ADMET profiling, and drug-likeness assessment, was employed to evaluate these bioactive compounds. Delphinidin emerged as the lead candidate, exhibiting the highest binding affinity with a docking energy of -8.6 kcal/mol, comparable to -8.9 kcal/mol of the known inhibitor T863, followed by cyanidin-3-sambubioside, cyanidin-3,5-diglucoside, delphinidin-3-sambubioside, and gossypitrin, which demonstrated binding energies of -8.4, -8.3, -8.1, and -8.1 kcal/mol, respectively. Pharmacokinetic and toxicological profiling confirmed delphinidin as the most promising lead due to its favourable drug-like properties. The stability of the delphinidin-DGAT complex was substantiated via 100 ns molecular dynamics simulations; furthermore, the structural stability and conformational dynamics of the complex under physiological conditions were validated using molecular mechanics-generalized born surface area free energy calculations and principal component analysis. Delphinidin demonstrated a highly favourable binding free energy of -74.79 kcal/mol, confirming the thermodynamic stability of the interaction. These findings suggest that delphinidin, derived from *Hibiscus sabdariffa*, serves as a promising potential therapeutic agent for the management of obesity.

Keywords: Molecular Docking, MD Simulation, Bioactive Compounds, Pharmacokinetic, and ADMET Studies
How to cite this article: Sharma S, Srivastava SK, Srivastava R. Computational Investigation of Bioactive Compounds from Hibiscus sabdariffa in Modulating TGA Biosynthesis: An Approach to Control Obesity. Int J Drug Deliv Technol. 2026;16(57s): 952-967. DOI: 10.25258/ijddt.16.57s.100
Source of support: Nil
Conflict of interest: None

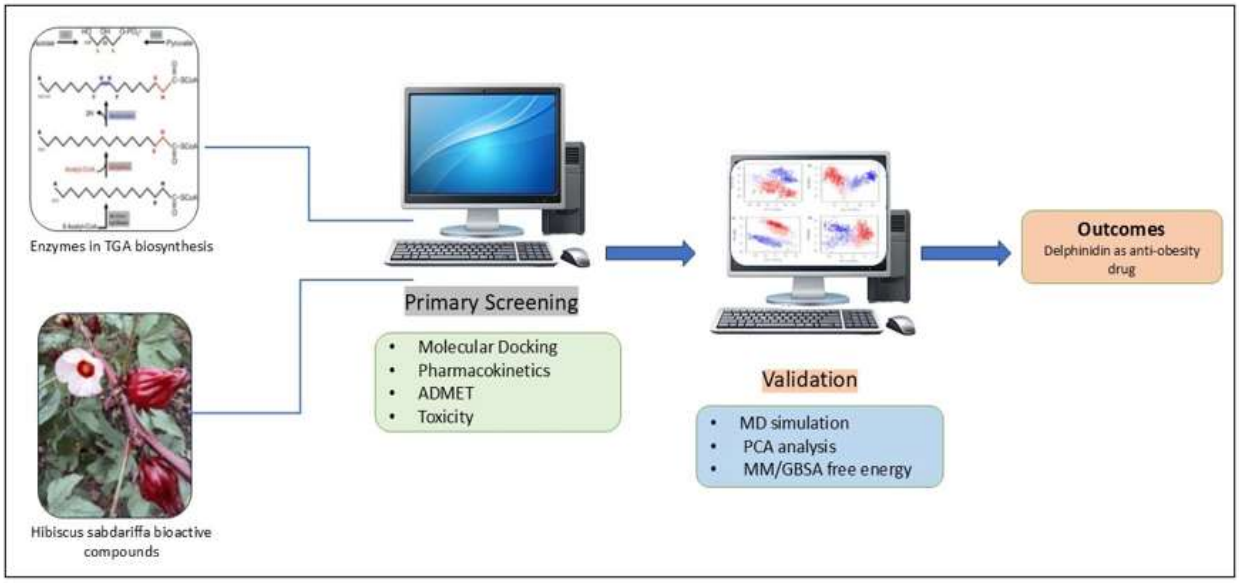

Corresponding Author: Sweta Sharma, shweta.sharma@iftmuniversity.ac.in

1. INTRODUCTION

Obesity is a metabolic disorder marked by excess body fat build up that poses a major global health threat due to its links to type 2 diabetes, heart disease, and certain cancers (Afolabi et al., 2023). Conventional treatments often exhibit limited efficacy and can be accompanied by adverse effects, thus driving the search for alternative therapeutic strategies (Adam et al., 2023). The known inhibitor T863 is a potent DGAT1 inhibitor (Cao et al., 2011), though DGAT1 inhibitors generally face challenges with clinical utility due to potential side effects and pharmacokinetic limitations (DeVita & Pinto, 2013), necessitating the exploration of alternative natural scaffolds. Natural products, particularly those derived from medicinal plants, offer a promising avenue for novel anti-obesity agents, with *Hibiscus sabdariffa* emerging as a prominent candidate (Palomo-Martínez et al., 2025). Various studies have demonstrated the anti-obesogenic potential of *Hibiscus sabdariffa*'s bioactive compounds, attributed to their pleiotropic effects on energy metabolism, lipid accumulation, and adipogenesis (Ojulari et al., 2019). Specifically, extracts from *Hibiscus sabdariffa* flowers have been shown to reduce lipid and triglyceride levels, and inhibit adipogenesis by modulating critical pathways such as phosphoinositide 3 kinase and mitogen-activated protein kinase (Davkova et al., 2024). Beyond these general effects, specific polyphenolic fractions from *Hibiscus sabdariffa* have demonstrated the capacity to inhibit triglyceride accumulation and mitigate oxidative stress and reduce the secretion of inflammatory adipokines that modulate macrophage infiltration in adipose tissue (Herranz-López et al., 2019). Furthermore, specific bioactive compounds within *Hibiscus sabdariffa* , such as hydrolysable and extractable polyphenols, have been identified as key contributors to its anti-obesity effects, targeting mechanisms like the inhibition of cytoplasmic lipid accumulation and adipogenic differentiation in preadipocytes (Amaya-Cruz et al., 2019; Tan & Ng, 2025). This suggests a need for further investigation into the precise molecular mechanisms by which these compounds exert their inhibitory effects on lipid metabolism and adipogenesis, particularly concerning triglyceride biosynthesis pathways. Indeed, previous research has indicated that *Hibiscus sabdariffa* extracts can effectively reduce body weight, BMI, body fat, and waist-to-hip ratio, alongside lowering serum free fatty acid levels and improving liver steatosis (Chang et al., 2014). Moreover, the anthocyanins present in *Hibiscus sabdariffa* extracts have demonstrated efficacy comparable to conventional treatments in protecting against high-fat diet-induced obesity, suggesting their crucial role in mediating these protective effects (Huang et al., 2015). The therapeutic potential of *Hibiscus sabdariffa* extends beyond its antioxidant properties, influencing lipid metabolism and fat absorption, thereby, modulating obesity through multiple mechanisms (Sheba & Ilakkia, 2016). Given its established safety profile and minimal side effects during long-term use, *Hibiscus sabdariffa* presents a compelling subject for advanced pharmacological inquiry into its anti-obesity mechanisms (Cancellara et al., 2024; Kim et al., 2025). This paper aims to elucidate the specific bioactive compounds within *Hibiscus sabdariffa* and their respective mechanisms of action in modulating triglyceride accumulation biosynthesis as a novel strategy for anti-obesity drug development.

2. MATERIALS AND METHODS

A comprehensive computational pipeline, integrating molecular docking, drug-likeness assessment, ADMET profiling, toxicity prediction, and molecular dynamics simulations, was developed to facilitate the discovery and validation of diacylglycerol acyltransferase inhibitors (Antypenko et al., 2025; Peng et al., 2024; Stefano et al., 2023).

2.1 Protein preparation and active site identification

The three-dimensional structure of DGAT (PDB ID: 8ESM) was obtained from the Protein Data Bank (PDB). The protein was complexed with an inhibitor WS0501. The amino acid residues TRP374, TRP377, ASN378, and SER411 were present at the binding site of it's, and were identified as the active site (Figure 1). Gaps in the structure, including missing residues, were rectified using MODELLER 10.8, yielding a complete model suitable for computational investigations (Kelm et al., 2010). Amino acid residues ranging from 1-65, 229-238, and 482-488 were added to prevent any interruption in further computational analysis. All water molecules and heteroatoms present in the structure were removed before docking. The protein structure was prepared by adding polar hydrogens using the Autodock Tool (ADT).

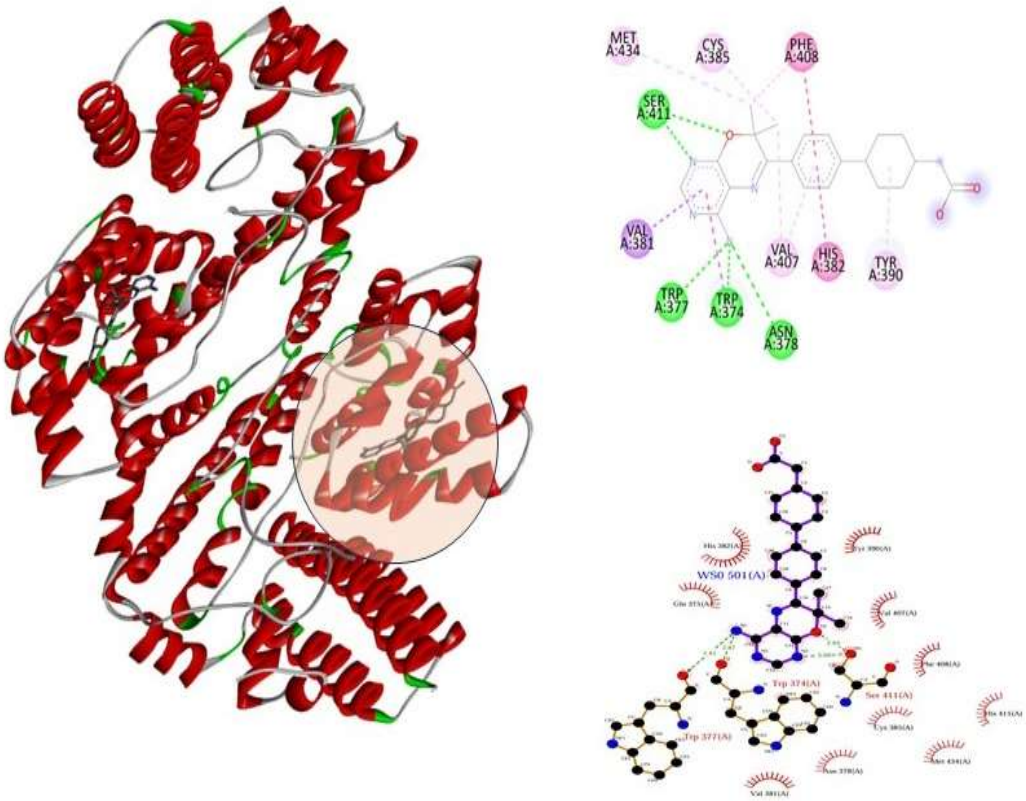

Figure 1: Three-dimensional structure of DGAT complexed with WS0501 and the amino acid residues interacting with ligands

2.2 Ligand Preparation and Optimization

A library of bioactive compounds specific to *Hibiscus sabdariffa* including anthocyanins, organic acids, phenolic acids, and flavonoids was curated. The structures of bioactive compounds were retrieved from PubChem in SDF format (Table 1). The ligands were converted to PDB files using PyMOL, energy-minimized using AutoDock Tools, saved in PDBQT format, and subsequently used for molecular docking. FDA-approved drugs orlistat, bupropion, and diethylpropion were downloaded from PubChem and prepared for molecular docking. These drugs were used as a standard for identifying potent inhibitors among the bioactive compounds.

Table 1 *Hibiscus sabdariffa* bioactive compounds with their CID, SMILES, and structures

S. No.	Chemical Name/ CID	SMILES	Structure
1.	Hibiscus acid 9856782	C(C(=O)O)[C@@](C@@H](C(=O)O)O)(C(=O)O)O	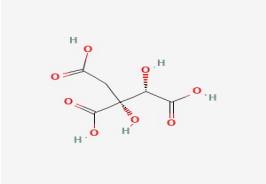

2.	Hydroxycitric acid 123908	C(C(=O)O)C(C(C(=O)O)O)(C(=O)O)O	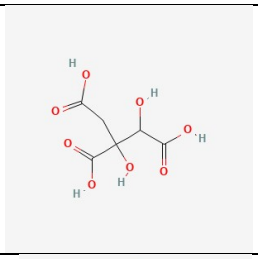
3.	Dimethyl hibiscus acid 139088440	CS(=O)C.C1C(=O)O[C@@H]([C@]1(C(=O)O)O)C(=O)O	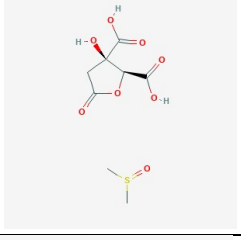
4.	Delphinidin 3-sambubioside 10196837	C1[C@H]([C@@H]([C@H]([C@@H](O1)O[C@@H]2[C@H]([C@@H]([C@H](O[C@H]2OC3=CC4=C(C=C(C=C4[O+]=C3C5=CC(=C(C(=C5)O)O)O)O)O)CO)O)O)O)O)O	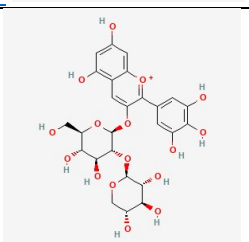
5.	Cyanidin-3-sambubioside 3084569	C1[C@H]([C@@H]([C@H]([C@@H](O1)O[C@@H]2[C@H]([C@@H]([C@H](O[C@H]2OC3=CC4=C(C=C(C=C4[O+]=C3C5=CC(=C(C=C5)O)O)O)O)CO)O)O)O)O)O.[Cl-]	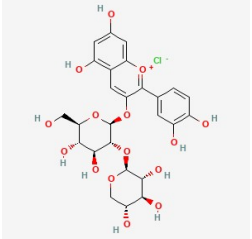
6.	Cyanidin-3,5-diglucoside 441688	C1=CC(=C(C=C1C2=C(C=C3C(=CC(=CC3=[O+]2)O)O[C@H]4[C@@H]([C@H]([C@@H]([C@H](O4)CO)O)O)O)O[C@H]5[C@@H]([C@H]([C@@H]([C@H](O5)CO)O)O)O)O)O	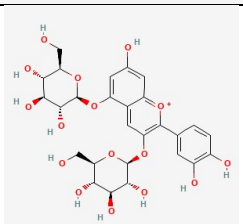
7.	Delphinidin 128853	C1=C(C=C(C(=C1O)O)O)C2=[O+]C3=CC(=CC(=C3C=C2O)O)O	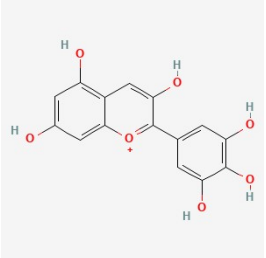

8.	Hibiscitrin 15559736	C1=C(C=C(C(=C1O)O)O)C2=C(C(=O)C3=C(O2)C(=C(C=C3O)O)O)OC4C(C(C(C(O4)CO)O)O)O	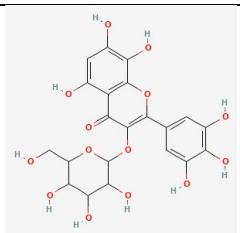
9.	Gossypitrin 6452123	C1=CC(=C(C=C1C2=C(C(=O)C3=C(O2)C(=C(C=C3O)O[C@H]4[C@@H]([C@H]([C@@H]([C@H](O4)CO)O)O)O)O)O)O)O	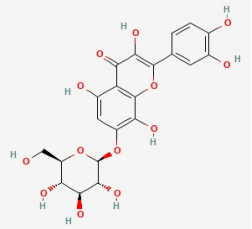
10.	Quercetin 5280343	C1=CC(=C(C=C1C2=C(C(=O)C3=C(C=C(C=C3O2)O)O)O)O)O	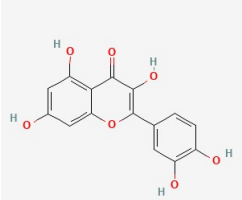
11.	Luteolin 5280445	C1=CC(=C(C=C1C2=CC(=O)C3=C(C=C(C=C3O2)O)O)O)O	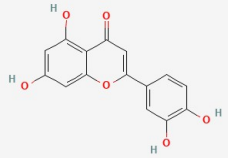
12.	Chlorogenic acid 1794427	C1[C@H]([C@H]([C@@H](C[C@@]1(C(=O)O)O)OC(=O)/C=C/C2=CC(=C(C=C2)O)O)O)O	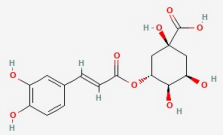
13.	Protocatechuic acid 72	C1=CC(=C(C=C1C(=O)O)O)O	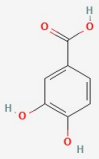
14.	P-Coumaric acid 637542	C1=CC(=CC=C1/C=C/C(=O)O)O	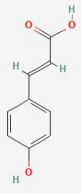

15.	Ferulic acid 445858	COC1=C(C=CC(=C1)/C=C/C(=O)O)O	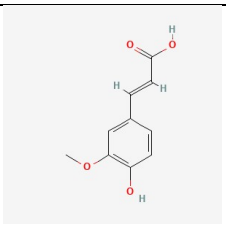
16.	Caffeic acid 689043	C1=CC(=C(C=C1/C=C/C(=O)O)O)O	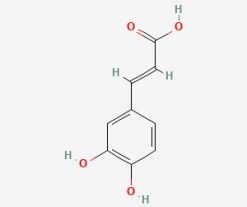
17.	Ellagic acid 5281855	C1=C2C3=C(C(=C1O)O)OC(=O)C4=CC(=C(C(=C43)OC2=O)O)O	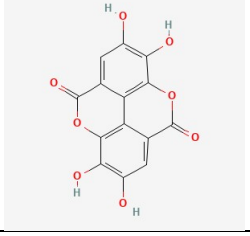

2.3 Molecular Docking

The AutoDock Vina application (version 1.2.3) was used to conduct docking studies. The grid box was positioned at the active site of the protein DGAT (coordinates: x = 133.267, y = 113.701, z = 99.361), with dimensions of x = 40, y = 40, z = 40. An energy range of 4 and exhaustiveness of 8 were set to determine the accurate placement of ligands. PyMOL was used to export the docked complexes, and Discovery Studio Visualizer was used to visualize the docking interactions.

2.4 Pharmacokinetic properties and Lipinski's rule of five

To evaluate the drug-likeness and pharmacokinetic profiles of the selected *Hibiscus sabdariffa* bioactive compounds, the Swiss-ADME platform was employed. This web-based computational tool is widely utilized in in silico drug discovery to estimate molecular properties essential for oral bioavailability, drug-likeness, and pharmacokinetics (Daina et al., 2017). Specifically, parameters defining Lipinski's rule of five including molecular weight, hydrogen bond donors and acceptors, Log P, and molar refractivity were calculated using structural data retrieved from the PubChem database. Furthermore, toxicity profiling was performed via the ProTox 3.0 server to verify that the identified lead candidates exhibit safety profiles comparable to existing clinical standards (Banerjee et al., 2024). This multifaceted computational framework aimed to establish in silico protocols for confirming lead compound stability and pharmacological efficacy through comprehensive ADMET screening (Ameji et al., 2023; Naithani & Guleria, 2024).

2.5 Molecular dynamics simulations

Maestro platform was used to perform Molecular dynamics (MD) simulations. The protein-ligand complex was imported and processed through the system builder, which generated a solvation box by incorporating water molecules and counter ions to establish the simulation environment. The system utilized TIP3 water with a buffer region of approximately 10 Å and was neutralized by adding sodium (Na+) ions and counter ions to simulate physiological conditions. The simulation, covering a duration of 100 ns, was conducted at 300 K using an NPT ensemble, with the temperature gradually equilibrated from 0 K to 300 K (Kumar et al., 2025). Finally, the resulting MD trajectory was analyzed using Maestro's simulation interaction diagram to assess ligand affinity toward the protein and changes in protein flexibility. To rigorously evaluate the dynamic stability and structural integrity of the protein–ligand complex, we computed the root-mean-square deviation (RMSD), root-mean-square fluctuation (RMSF), radius of gyration (Rg), and solvent-accessible surface area (SASA) from the MD simulation trajectories. These metrics collectively characterize the conformational stability, residue-level flexibility, overall compactness, and solvent exposure of the system, providing robust evidence for the binding persistence of the inhibitor within the active site.

2.6 PCA and MM/GBSA Analysis

Principal Component Analysis was performed to characterize the system's energetic landscape and dominant conformational motions. Binding free energies were computed utilizing the Molecular Mechanics/Generalized Born Surface Area (MM/GBSA) approach. Furthermore, trajectory analysis was conducted to assess structural variations, with representative conformations identified from the simulation data (Kumar et al., 2025).

3. RESULTS AND DISCUSSION

Molecular docking of *Hibiscus sabdariffa* derived compounds was conducted against DGAT to assess their potential inhibitory capacity. Table 2 represents the docking scores and corresponding molecular interactions for the top-scoring compounds. The docked complexes are stabilized primarily through hydrogen bonds, Van der Waals forces, and various π-mediated interactions, including π-π, π-stacking, π-alkyl, and π-sulphur bonds. In the 2D interaction diagrams, these features are represented by specific colour coding: Van der Waals interactions in green, hydrogen bonds in light green, π-π-sulphur interactions in yellow, π-alkyl interactions in purple, and π-π stacking interactions in pink (Rashid et al., 2026).

Compounds were ranked based on their binding energy. Those exhibiting the lowest binding energies were identified as potential leads for inhibiting TGA biosynthesis (Figure 2), indicating a high potential for the development of anti-obesity therapeutics.

The study concluded that Delphinidin, Cyanidin 3-sambubioside, Cyanidin-3,5-diglucoside, Delphinidin 3-sambubioside, and Gossypitrin are the top-scoring docked molecules with binding energies of -8.6, -8.4, -8.3, -8.1, and -8.1 kcal/mol (Table 2).

Delphinidin, a natural anthocyanin, demonstrated a robust binding affinity of -8.6 kcal/mol, characterized by interactions with amino acid residues ASN378, HIS382, PHE408, TRP374, and VAL381. Cyanidin 3-sambubioside exhibited a binding energy of-8.4 kcal/mol, interacting with protein residues TRP334, TRP377, SER411, GLN465, and ASN378. Cyanidin-3,5-diglucoside showed binding by forming three critical hydrogen bonds with TRP377, ASN378, and SER411 residues within the DGAT active site. Delphinidin 3-sambubioside displayed a binding affinity of-8.1 kcal/mol, maintaining stability through strong interactions with CYS385, SER411, ASN378, GLN292, ASN330, HIS415, and PRO466. Gossypitrin, a natural flavonoid, also showed a favorable binding energy of-8.1 kcal/mol, engaging in key hydrophobic and hydrogen-bonding interactions with catalytic residues THR371, TRP374, ARG404, and VAL407, highlighting its potential as a lead candidate for therapeutic intervention.

The binding energies and interaction sites of these bioactive compounds were compared against those of FDA-approved drugs and the known inhibitor T863 (Table 3). The analysis demonstrated that Delphinidin, Cyanidin 3-sambubioside, Cyanidin-3,5-diglucoside, Delphinidin 3-sambubioside, and Gossypitrin exhibited superior docking scores compared to the reference drug and T863 inhibitor.

Table 2: Molecular docking studies, binding energies, and interactions of bioactive compounds with DGAT

S. No	Bioactive Compounds	Binding Energy (kcal/mol)	Amino acid interactions	Number of Hydrogen bonds
1.	Hibiscus acid	-5.3	ARG212, ASP213, SER216, ARG220	4
2.	Hydroxycitric acid	-5.3	SER216, TRP217, ARG220, PRO392	4
3.	Dimethyl hibiscus acid	-5.5	SER216, TRP217, ARG220, PRO392	4
4.	**Delphinidin 3-sambubioside**	**-8.1**	**CYS385, SER411, ASN378, TRP377, VAL381**	**3**
5.	**Cyanidin 3-sambubioside**	**-8.4**	**GLN292, ASN330, HIS415, PRO466, VAL419**	**4**

6.	**Cyanidin-3,5-diglucoside**	**-8.3**	**TRP334, TRP377, SER411, GLN465, ASN378**	**4**
7.	**Delphinidin**	**-8.6**	**ASN378, HIS382, PHE408, TRP374, VAL381**	**1**
8.	Hibiscitrin	-7.9	ASN330	1
9.	**Gossypitrin**	**-8.1**	**THR371, TRP374, ARG404, VAL407**	**2**
10.	Quercetin	-7.8	GLN460, PRO466	2
11.	Luteolin	-8.0	TRP377, HIS382	2
12.	Chlorogenic acid	-7.8	THR371, TRP377	2
13.	Protocatechuic acid	-5.6	TRP377, ASN378	2
14.	Coumaric acid	-6.6	—	0
15.	Ferulic acid	-6.3	THR371, GLN375	2
16.	Caffeic acid	-6.2	SER411	1
17.	Ellagic acid	-7.4	ASN378	1

Table 3: Binding energy of FDA-approved drugs and inhibitor T863 with DGAT

S. No.	Drugs/ Inhibitor	Binding Energy (kcal/mol)
1	Bupropion	-6.9
2	Diethylpropion	-6.9
3	Orlistat	-6.2
4	**T863**	**-8.9**

To further elucidate the potential of the identified bioactive compounds, their pharmacokinetic profiles, compliance with Lipinski's rule of five, and toxicological properties were assessed (Tables 4, 5, and 6). The analysis indicated that among the five selected candidates, only Delphinidin complied with Lipinski's rule of five, possessing a molecular weight of 338.7 g/mol, 7 hydrogen bond acceptors, 5 hydrogen bond donors, and a LogP value of -0.382. Additionally, the pharmacokinetic profile suggested favorable gastrointestinal absorption, low blood-brain barrier permeability, and a lack of carcinogenic potential (Sharma et al., 2021). These findings are consistent with prior computational screenings where phytochemicals exhibiting favorable binding affinities and safety profiles were validated for their drug-like characteristics (Rashid et al., 2026). Moreover, toxicity evaluations and lead-likeness assessments were conducted to confirm that the molecule does not exhibit mutagenic effects, further supporting its viability as a therapeutic candidate. The water solubility of selected bioactive compounds also suggested Delphinidin as a good lead candidate for an anti-obesity drug (Table 7). Consistent with successful

screenings of other plant-derived inhibitors, these results emphasize the necessity of integrating rigorous ADMET profiling with docking energies to ensure potential candidates remain viable for subsequent clinical development.

Table 4: Lipinski's Properties of Bioactive Compounds

Compounds	Molecular weight (g/mol)	XLogP	H-bond acceptors	H-bond donors	Rotatable bonds
Hibiscus acid	268.24	-1.803	8	3	2
Hydroxycitric acid	208.12	-2.278	8	5	5
Dimethyl hibiscus acid	268.24	-1.803	8	3	2
Delphinidin 3-sambubioside	597.5	-1.449	16	11	6
Cyanidin-3-sambubioside	616.95	-4.151	15	10	6
Cyanidin-3,5-diglucoside	646.98	-5.141	16	11	7
Delphinidin	338.7	-0.382	7	5	1
Hibiscitrin	496.38	-1.128	14	10	4
Gossypitrin	480.38	-0.833	13	9	4
Quercetin	302.24	1.988	7	5	1
Luteolin	286.24	2.2824	6	4	1
Chlorogenic acid	354.31	-0.646	9	6	5
Protocatechuic acid	168.15	1.1044	4	3	1
P-Coumaric acid	164.16	1.49	3	2	2
Ferulic acid	194.18	1.4986	4	2	3
Caffeic acid	180.16	1.1956	4	3	2
Ellagic acid	302.19	1.3128	8	4	0

Table 5: Pharmacokinetics profile of bioactive compounds identified as potential inhibitors

Bioactive compounds	GI absorption	BB permeation	P-gp substrate	Cytochrome P450 inhibitors				
				CYP1A2	CYP2C19	CYP2C9	CYP2D6	CYP3A4
Delphinidin	High	No	Yes	No	No	No	No	No
Cyanidin 3-sambubioside	High	No	No	No	No	No	No	No
Cyanidin-3,5-diglucoside	High	No	Yes	Yes	No	No	No	No
Delphinidin 3-sambubioside	High	No	Yes	No	No	No	No	No
Gossypitrin	High	No	No	No	No	No	No	No

Table 6: Predicted toxicity of bioactive compounds identified as potential inhibitors

Bioactive compounds	Hepatotoxicity	Neurotoxicity	Nephrotoxicity	Cardiotoxicity	Carcinogenicity	Immunotoxicity	Mutagenicity	Cytotoxicity
Delphinidin	Inactive	Inactive	Active	Inactive	Inactive	Inactive	Inactive	Inactive
Cyanidin 3-sambubioside	Inactive	Inactive	Active	Inactive	Active	Inactive	Inactive	Inactive
Cyanidin-3,5-diglucoside	Inactive	Inactive	Active	Inactive	Inactive	Inactive	Inactive	Inactive
Delphinidin 3-sambubioside	Inactive	Inactive	Active	Inactive	Inactive	Inactive	Inactive	Inactive
Gossypitrin	Inactive	Inactive	Active	Inactive	Active	Inactive	Active	Active

Table 7: Water solubility and medicinal chemistry suitability of bioactive compounds

Bioactive compounds	Water solubility	PAINS alerts	Synthetic Accessibility
Delphinidin	Soluble	Absent	3.18
Cyanidin 3-sambubioside	Soluble	Absent	3.15
Cyanidin-3,5-diglucoside	Soluble	Absent	3.18
Delphinidin 3-sambubioside	Very soluble	Absent	3.18
Gossypitrin	Soluble	Absent	3.02

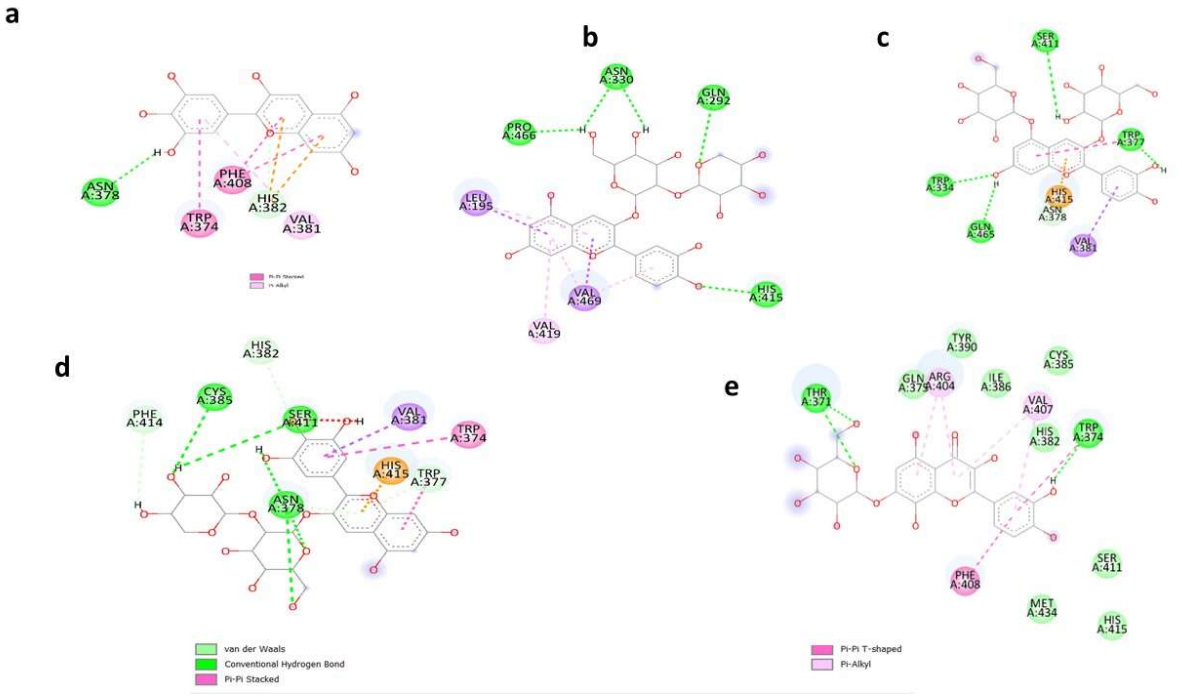

Figure 2: Molecular docking interactions of DGAT with ligands (a) Binding residues of delphinidin, (b) Cyanidin 3-sambubioside, (c) Cyanidin-3,5-diglucoside, (d) Delphinidin 3-sambubioside, and (e) gossypitrin

To investigate the dynamic behaviour and stability of the protein-ligand complex, a 100 ns MD simulation was performed (Akinola et al., 2025). The root-mean-square deviation trajectories for both the protein and ligand within the DGAT–delphinidin complex are presented in Figure 3. The protein RMSD profile reached a steady state after approximately 23 ns, with fluctuations stabilizing around 2.6 Å for the remainder of the simulation. Concurrently, the ligand RMSD showed minimal deviation following 25 ns, maintaining a consistent range of 0.6–1.6 Å, suggesting that delphinidin retained a stable binding conformation within the active site. The initial 25 ns equilibration period, characterized by significant conformational rearrangements, was likely attributable to the inherent structural flexibility of the delphinidin ligand.

Figure 3 illustrates the residue-specific flexibility of the DGAT–delphinidin complex through an RMSF plot. The protein residues predominantly exhibited low RMSF values of approximately 2.2 Å, signifying overall structural rigidity. In particular, the active site residues showed minimal fluctuations (<2.0 Å), underscoring the stability of the complex during ligand binding. Conversely, higher RMSF values in loop (residues 1-61 & 150-175) and terminal regions were consistent with their inherent

flexibility, confirming a robust and persistent interaction between delphinidin and the DGAT binding pocket.

This analysis allows the calculation of structural stability parameters such as RMSD, RMSF, and the radius of gyration, which are essential for validating the resilience of the lead compound within the binding pocket (Choudhary et al., 2023). Specifically, the RMSD profiles of the complex provide critical insights into the conformational equilibrium maintained by the ligand during the simulation (Rahman et al., 2024). Furthermore, the RMSF values offer a detailed mapping of protein flexibility across the active site residues, confirming that the identified ligands effectively stabilize the enzyme structure during the 100 ns trajectory (Akash et al., 2023).

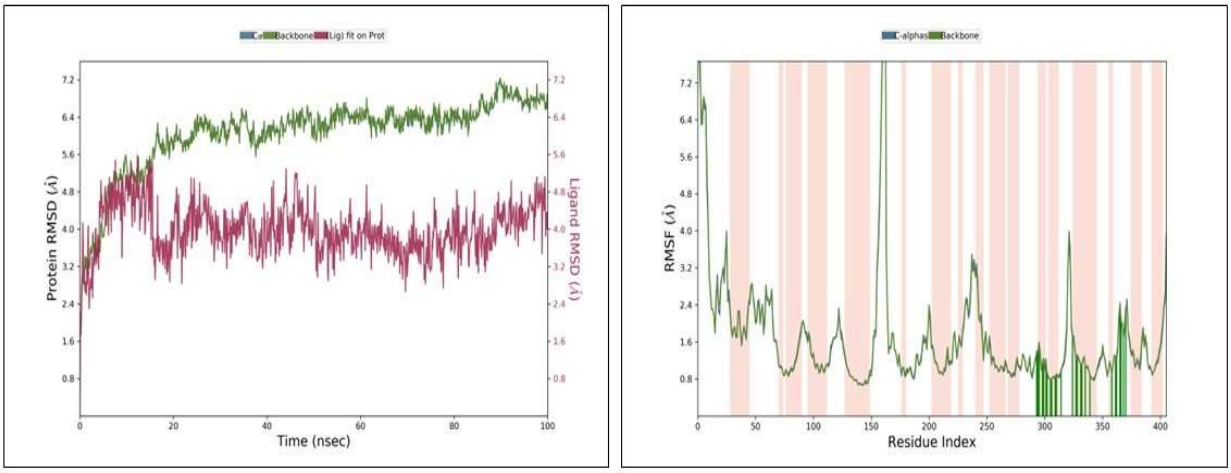

Figure 3: Root mean square deviation (RMSD) and Root mean square fluctuation (RMSF) of DGAT-delphinidin complex

The stacked bar chart depicted in Figure 4 provides a summary of the contact profile and interactions between delphinidin and the DGAT active site residues throughout the simulation. The observed interactions primarily comprised of hydrogen bonds, water bridges, ionic interactions, and hydrophobic contacts (Allegra et al., 2021) Specifically, residues THR371, TRP374, ASN378, HIS382, VAL407, and SER411 were characterized as key participants, establishing stable hydrogen bonds throughout the MD trajectory.

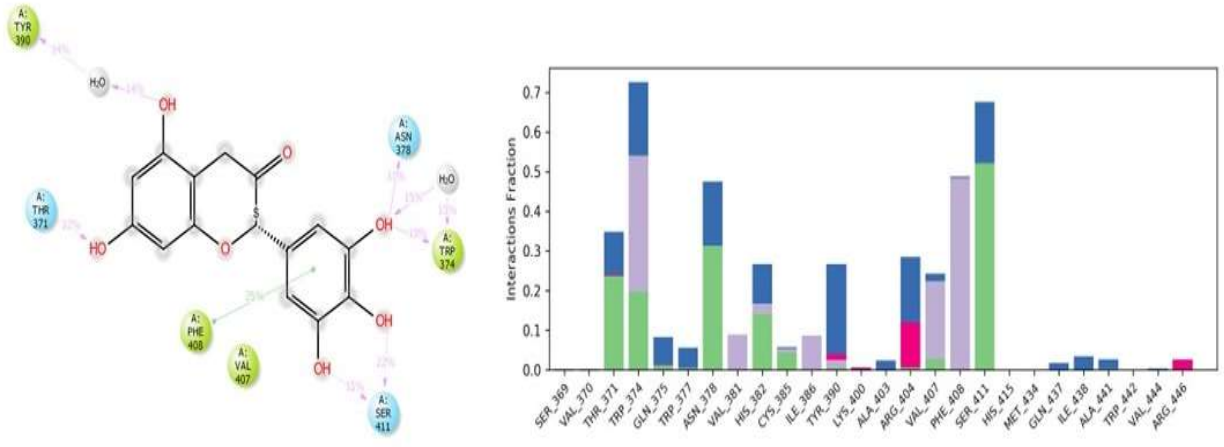

Figure 4: The bar chart depicting the interaction between delphinidin and DGAT throughout the 100 ns MD Simulation

The MM/GBSA binding free energy analysis for the DGAT–delphinidin complex, illustrated in Figure 5, provides detailed insights into the thermodynamic stability and binding affinity of the ligand within the enzyme's active site. The calculated total binding free energy of −74.7934 kcal/mol signifies a robust interaction between delphinidin and DGAT. Furthermore, the decomposition of the energy components revealed that Van der Waals forces (−50.2987 kcal/mol) and lipophilic contributions (−30.0320 kcal/mol) were the primary drivers of the binding process, underscoring the critical role of nonpolar contacts in stabilizing the complex.

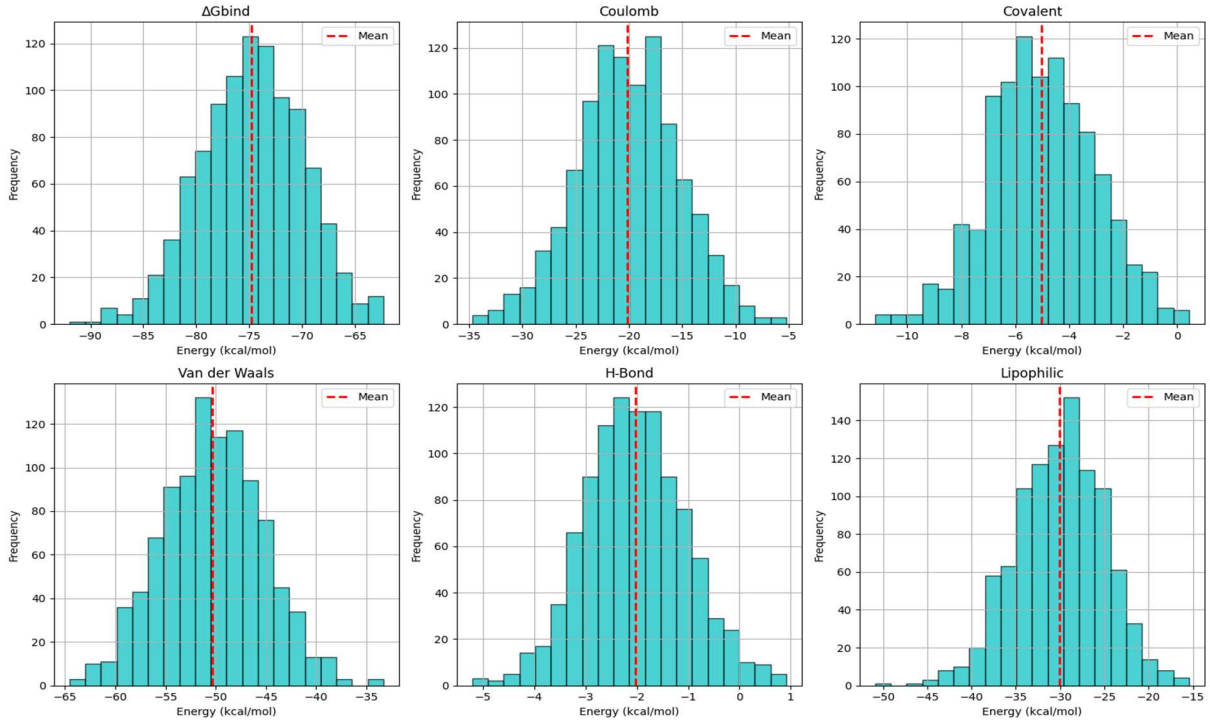

Figure 5: MM/GBSA binding free energy analysis of the complex formed between DGAT–delphinidin

To elucidate the conformational dynamics of the DGAT–delphinidin complex throughout the molecular dynamics trajectory, a Principal Component Analysis was employed (Figure 6). The three-dimensional projection of the first three principal components demonstrates distinct clustering along the PC1 axis, signifying a continuous and stable transition between conformational ensembles, thereby corroborating the enduring structural stability of the protein–ligand interaction.

The 3D free energy landscape analysis provides significant insights into the conformational dynamics and stability of the DGAT–delphinidin complex, with energy minima identifying the most thermodynamically stable configurations. As depicted in Figure 6, the landscape reveals well-defined energy basins and a scarcity of energetic barriers, confirming the existence of stable conformers that exhibit minimal structural fluctuations throughout the simulation (Kumar et al., 2025).

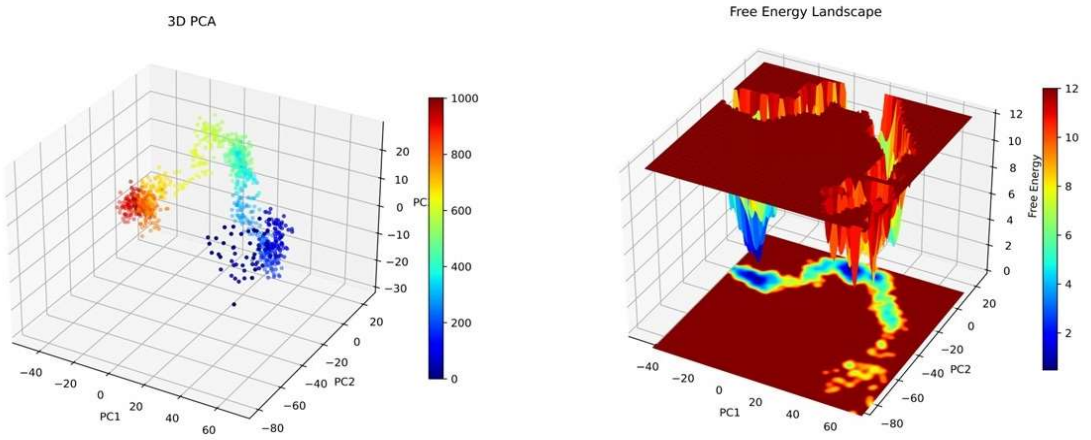

Figure 6: Three-Dimensional principal component analysis (PCA) of molecular dynamics simulation trajectories and 3D Free Energy Landscape (FEL) analysis based on PCA projections of DGAT-delphinidin complex.

CONCLUSION

The integration of *Hibiscus sabdariffa* bioactive compounds as potent enzyme inhibitors represents a significant advancement in the development of sustainable, plant-based anti-obesity therapies. Computational investigations confirm that these phytochemicals, particularly Delphinidin, Cyanidin 3-sambubioside, Cyanidin-3,5-diglucoside, Delphinidin 3-sambubioside, and Gossypitrin, are the top-scoring docked molecules with binding energies of -8.6, -8.4, -8.3, -8.1, and -8.1 kcal/mol. Delphinidin, exhibiting a high binding stability demonstrates promising pharmacokinetic profiles and minimal toxicity. Molecular dynamics simulations further substantiate these findings, revealing that delphinidin, a lead compound maintains stable interactions and conformational equilibrium within the active site throughout the simulation period. Ultimately, the persistence of these protein-ligand contacts, verified through rigorous MD analysis, underscores the therapeutic efficacy and structural durability of *Hibiscus sabdariffa* derivatives in modulating TGA biosynthesis.

Acknowledgements:

The authors wish to acknowledge IFTM University, Moradabad, for the support and encouragement throughout the research and facilities provided for the successful completion of this computational investigation.

Disclosure Statement:

The authors declare no conflict of interest. The authors did not receive any funding for this work.

REFERENCES

1. Adam, S. H., Abu, I. F., Kamal, D. A. M., Febriza, A., Kashim, M. I. A. M., & Mokhtar, M. H. (2023). A Review of the Potential Health Benefits of Nigella sativa on Obesity and Its Associated Complications. Plants, 12(18), 3210–3210. https://doi.org/10.3390/plants12183210

2. Afolabi, H. A., Zakarıa, Z., Salleh, M. S. M., Ch'ng, E. S., Nafi, S. N. M., Aziz, A. A. A., Al-Mhanna, S. B., Irekeola, A. A., Wada, Y., & Abubakar, B. D. (2023). Obesity: A Prerequisite for Major Chronic Illnesses. In IntechOpen eBooks. IntechOpen. https://doi.org/10.5772/intechopen.111935

3. Akash, S., Bayıl, İ., Rahman, Md. A., Mukerjee, N., Maitra, S., Islam, Md. R., Rajkhowa, S., Ghosh, A., Al-Hussain, S. A., Zaki, M. E. A., Jaiswal, V., Sah, S., Barboza, J. J., & Sah, R. (2023). Target specific inhibition of West Nile virus envelope glycoprotein and methyltransferase using phytocompounds: an in silico strategy leveraging molecular docking and dynamics simulation. Frontiers in Microbiology, 14. https://doi.org/10.3389/fmicb.2023.1189786

4. Akinola, L. K., Abdalla, M., Abubakar, H., Abubakar, K., Rabiu, S. M., Rufai, M., & Umar, N. Z. (2025). In silico discovery of new ornithine decarboxylase inhibitor with potential for human African trypanosomiasis treatment. Discover Chemistry., 2(1). https://doi.org/10.1007/s44371-025-00113-2

5. Allegra, M., Tutone, M., Tesoriere, L., Attanzio, A., Culletta, G., & Almerico, A. M. (2021). Evaluation of the IKKβ Binding of Indicaxanthin by Induced-Fit Docking, Binding Pose Metadynamics, and Molecular Dynamics. Frontiers in Pharmacology, https://doi.org/10.3389/fphar.2021.701568

6. Amaya-Cruz, D. M., Pérez-Ramírez, I. F., Pérez-Jiménez, J., Nava, G. M., & Reynoso-Camacho, R. (2019). Comparison of the bioactive potential of Roselle (*Hibiscus*

sabdariffa L.) calyx and its by-product: Phenolic characterization by UPLC-QTOF MS and their anti-obesity effect in vivo. Food Research International, 126, 108589–108589. https://doi.org/10.1016/j.foodres.2019.108589

7. Ameji, J. P., Uzairu, A., Shallangwa, G. A., & Uba, S. (2023). Design, pharmacokinetic profiling, and assessment of kinetic and thermodynamic stability of novel anti-Salmonella typhi imidazole analogues. Bulletin of the National Research Centre/Bulletin of the National Research Center, 47(1). https://doi.org/10.1186/s42269-023-00983-5

8. Antypenko, L., Shabelnyk, K., Antypenko, O., Arisawa, M., Kamyshnyi, O., Oksenych, V., & Коваленко, С. І. (2025). In Silico Identification and Characterization of Spiro[1,2,4]triazolo[1,5-c]quinazolines as Diacylglycerol Kinase α Modulators. Molecules, 30(11), 2324–2324. https://doi.org/10.3390/molecules30112324

9. Banerjee, P., Kemmler, E., Dunkel, M., & Preißner, R. (2024). ProTox 3.0: a webserver for the prediction of toxicity of chemicals. Nucleic Acids Research, 52. https://doi.org/10.1093/nar/gkae303

10. Cancellara, R. J. S., Freitas, A. C. de, & Oliveira, B. (2024). Benefícios do tratamento com *Hibiscus sabdariffa* para a obesidade, doenças associadas e seus efeitos adversos. Revista Brasileira de Plantas Medicinais, 21(3), 192–200. https://doi.org/10.70151/zra53r95

11. Cao, J., Zhou, Y., Peng, H., Huang, X., Stahler, S. L., Suri, V., Qadri, A., Gareski, T., Jones, J. E., Hahm, S., Perreault, M., McKew, J. C., Shi, M., Xu, X., Tobin, J. F., & Gimeno, R. E. (2011). Targeting Acyl-CoA:Diacylglycerol Acyltransferase 1 (DGAT1) with Small Molecule Inhibitors for the Treatment of Metabolic Diseases. Journal of Biological Chemistry, 286(48), 41838–41851. https://doi.org/10.1074/jbc.m111.245456

12. Chang, H.-C., Peng, C., Yeh, D., Kao, E., & Wang, C. (2014). *Hibiscus sabdariffa* extract inhibits obesity and fat accumulation, and improves liver steatosis in humans. Food & Function, 5(4), 734–734. https://doi.org/10.1039/c3fo60495k

13. Choudhary, S., Kesavan, A. K., Juneja, V. K., & Thakur, S. (2023). Molecular modeling, simulation and docking of Rv1250 protein from Mycobacterium tuberculosis. Frontiers in Bioinformatics, 3. https://doi.org/10.3389/fbinf.2023.1125479

14. Daina, A., Michielin, O., & Zoete, V. (2017). SwissADME: a free web tool to evaluate pharmacokinetics, drug-likeness and medicinal chemistry friendliness of small molecules. Scientific Reports, 7(1). https://doi.org/10.1038/srep42717

15. Davkova, I., Zhivikj, Z., Kukić, J., Cvetkovik-Karanfilova, I., Stefkov, G., Kulevanova, S., & Karapandzova, M. (2024). Natural products in the management of obesity. Arhiv Za Farmaciju, 74(3), 298–315. https://doi.org/10.5937/arhfarm74-50438

16. DeVita, R. J., & Pinto, S. (2013). Current Status of the Research and Development of Diacylglycerol O-Acyltransferase 1 (DGAT1) Inhibitors. Journal of Medicinal Chemistry, 56(24), 9820–9825. https://doi.org/10.1021/jm4007033

17. Herranz-López, M., Olivares-Vicente, M., Boix-Castejón, M., Caturla, N., Roche, E., & Micol, V. (2019). Differential effects of a combination of *Hibiscus sabdariffa* and Lippia citriodora polyphenols in overweight/obese subjects: A randomized controlled trial. Scientific Reports, 9(1). https://doi.org/10.1038/s41598-019-39159-5

18. Huang, T.-W., Chang, C., Kao, E., & Lin, J. (2015). Effect of*Hibiscus sabdariffa* extract on high fat diet–induced obesity and liver damage in hamsters. Food & Nutrition Research, 59(1), 29018–29018. https://doi.org/10.3402/fnr.v59.29018

19. Kelm, S., Shi, J., & Deane, C. M. (2010). MEDELLER: homology-based coordinate generation for membrane proteins. Bioinformatics, 26(22), 2833–2840. https://doi.org/10.1093/bioinformatics/btq554

20. Kim, S., Shin, H.-L., Son, T. H., Kim, D., Kwon, H., Shin, H., Park, Y., & Choi, S. (2025). Hibiscus syriacus Bud 'Pyeonghwa' Water Extract Inhibits Adipocyte Differentiation and Mitigates High-Fat-Diet-Induced Obesity In Vivo. International Journal of Molecular Sciences, 26(20), 9870–9870. https://doi.org/10.3390/ijms26209870

21. Kumar, R. C. S., Jayaraman, A., & Venkatachalapathy, R. (2025). Computational investigation of lignans as potential target for non-alcoholic fatty liver disease: Insights from network pharmacology, docking, DFT, and dynamics simulation analysis. Human Gene, 46, 201457–201457. https://doi.org/10.1016/j.humgen.2025.201457

22. Naithani, U., & Guleria, V. (2024). Integrative computational approaches for discovery and evaluation of lead compound for drug design. Frontiers in Drug Discovery, 4. https://doi.org/10.3389/fddsv.2024.1362456

23. Ojulari, O. V., Lee, S. G., & Nam, J. (2019). Beneficial Effects of Natural Bioactive Compounds from *Hibiscus sabdariffa* L. on Obesity. Molecules, 24(1), 210–210. https://doi.org/10.3390/molecules24010210

24. Palomo-Martínez, L. E., Paniagua-Castro, N., Escalona-Cardoso, G., Leyva-Daniel, D. E., Ibáñez-Hernández, M. Á., Cruz-Narváez, Y., & Alamilla-Beltrán,

L. (2025). Anti-Obesity Effect of Liposomal Suspension and Extracts of Hibiscus sabdariffa and Zingiber officinale in a Murine Model Fed a Hypercaloric Diet. Nutrients, 17(14), 2275–2275. https://doi.org/10.3390/nu17142275

25. Peng, C., Zhang, X., Zhang, L., Yang, A., Wang, Y., & Chen, X. (2024). Integration of molecular docking and molecular dynamics simulations with subtractive proteomics approach to identify the novel drug targets and their inhibitors in Streptococcus gallolyticus. Scientific Reports, 14(1). https://doi.org/10.1038/s41598-024-64769-z

26. Rahman, Md. S., Hosen, Md. E., Faruqe, M. O., Khalekuzzaman, M., Islam, M. A., Acharjee, U. K., Jardan, Y. A. B., Nafidi, H., Mekonnen, A. B., Bourhia, M., & Zaman, R. (2024). Evaluation of Adenanthera pavonina-derived compounds against diabetes mellitus: insight into the phytochemical analysis and in silico assays. Frontiers in Molecular Biosciences, 10. https://doi.org/10.3389/fmolb.2023.1278701

27. Rashid, L., Tasnim, J., Hasan, Md. M., Ismail, H., Hossain, K. R., Sarker, S., Younas, A., Mujtaba, M., & Alam, M. T. (2026). Computational screening of Sophora flavescens phytochemicals as potential aromatase inhibitors: Molecular docking, ADMET, Network pharmacology, Molecular dynamics simulation, and DFT studies. Pharmaceutical Science Advances, 4, 100108–100108. https://doi.org/10.1016/j.pscia.2026.100108

28. Sharma, A., Choi, H., Kim, Y., & Lee, H. (2021). Delphinidin and Its Glycosides' War on Cancer: Preclinical Perspectives. International Journal of Molecular Sciences, 22(21), 11500–11500. https://doi.org/10.3390/ijms222111500

29. Sheba, L. A., & Ilakkia, A. (2016). Anti-obesity effect of Hibiscus sabdariffa l.- a review. International Journal of Pharma and Bio Sciences, 7(4). https://doi.org/10.22376/ijpbs.2016.7.4.b341-345

30. Stefano, M. D., Masoni, S., Bononi, G., Poli, G., Galati, S., Gado, F., Manzi, S., Vagaggini, C., Brai, A., Caligiuri, I., Asif, K., Rizzolio, F., Macchia, M., Chicca, A., Sodi, A., Bussolo, V. D., Minutolo, F., Meier, P., Gertsch, J., Tuccinardi, T. (2023). Design, synthesis, ADME and biological evaluation of benzyl piperidine and benzylpiperazine derivatives as novel reversible monoacylglycerol lipase (MAGL) inhibitors. European Journal of Medicinal Chemistry, 263, 115916–115916. https://doi.org/10.1016/j.ejmech.2023.115916

31. Tan, S.-P., & Ng, W.-N. (2025). Malaysian Herbaceous and Shrub Species with Anti-Obesity Properties: A Review Records of Natural Products, 3, 204–238. ACG Publications. https://doi.org/10.25135/rnp.512.2412.3385